IEEE Access
Multidisciplinary | Rapid Review | Open Access Journal

Received 5 June 2023, accepted 8 June 2023, date of publication 13 June 2023, date of current version 22 June 2023.

Digital Object Identifier 10.1109/ACCESS.2023.3285792

RESEARCH ARTICLE

A Transformerless Photovoltaic Inverter With Dedicated MPPT for Grid Application

ALLAMSETTY HEMA CHANDER[1], K. DHANANJAY RAO[2], BANKUPALLI PHANI TEJA[3], LALIT KUMAR SAHU[4], (Member, IEEE), SUBHOJIT DAWN[2], FAISAL ALSAIF[5], SAGER ALSULAMY[6], AND TAHA SELIM USTUN[7], (Member, IEEE)

[1]Department of Electrical and Electronics Engineering, National Institute of Technology Puducherry, Karaikal 609605, India
[2]Department of Electrical and Electronics Engineering, Velagapudi Ramakrishna Siddhartha Engineering College, Vijayawada 520007, India
[3]Department of Electrical and Electronics Engineering, SRM Institute of Science and Technology, Kattankulathur, India
[4]Department of Electrical Engineering, National Institute of Technology Raipur, Raipur 492010, India
[5]Department of Electrical Engineering, College of Engineering, King Saud University, Riyadh 11421, Saudi Arabia
[6]Energy and Climate Change Division, Sustainable Energy Research Group, Faculty of Engineering and Physical Sciences, University of Southampton, SO16 7QF Southampton, U.K.
[7]Fukushima Renewable Energy Institute (FREA), National Institute of Advanced Industrial Science and Technology (AIST), Koriyama 963-0298, Japan

Corresponding authors: Taha Selim Ustun (selim.ustun@aist.go.jp) and K. Dhananjay Rao (kdhananjayrao@gmail.com)

This work was supported by the Researchers Supporting Project number (RSPD2023R646), King Saud University, Riyadh, Saudi Arabia.

ABSTRACT The objective of reducing the size and cost of the grid-connected photovoltaic system has led to advancements in the field of transformerless grid-connected inverters and gained high popularity in recent years. However, in such systems, the major limitation lies in realizing maximum power from individual modules. In this regard, this paper proposes a modular transformerless grid-connected photovoltaic multilevel inverter that realizes the individual maximum power point (MPP) of each module under different operating scenarios. The presented configuration is simple and modular, providing flexibility to increase the number of inputs with less component count. A single-phase synchronous reference frame PI (SRF-PI) controller has been designed and realized for the proposed system. The systematic procedure for designing the controller has been detailed. The converter and controller allow the system to realize individual MPP of the modules and simultaneously achieve the load demand maintaining the desired grid voltage. This has been verified under different operating scenarios in the MATLAB/Simulink environment. The same has been validated on a 300W laboratory prototype under source and load intermittencies. The proposed configuration has been compared with the similar works reported in the literature and it has been observed that it employs only 18 components. Also, the efficiency of the converter has been observed in the range of 89-95%. Further, the common-mode voltage and the leakage current have been measured to verify their suitability for grid-connected systems as per German VDE 0126-1-1 standards.

INDEX TERMS MPP, transformerless inverter, multilevel inverter, photovoltaic.

I. INTRODUCTION

The grid-connected solar photovoltaic (PV) systems throughout the globe tremendously support the generation system to meet the energy demand [1], [2]. In most developing countries, rooftop/ residential single-phase photovoltaic systems connected to the grid are gaining high popularity [3], [4], [5]. Different power converters have been gaining importance for integrating rooftop/residential systems into the grid [6]. The classical topological structure relates to a single-phase centralized transformerless inverter with a string of PV modules connected to the centralized inverter without a transformer. Two-stage conversion topologies with the initial DC/DC conversion followed by DC/AC conversion have been proposed in the literature with the transformerless operation. For instance, the inverting stage may comprise buck-type as H-5, HERIC, H6, or buck-boost type [7]. The H6 topologies and their modified works have also been reported in [6]. Due to higher efficiency and low cost, the family of string inverters has been commercialized on a larger scale.

The associate editor coordinating the review of this manuscript and approving it for publication was Bidyadhar Subudhi.

However, these topologies do not possess maximum power point tracking (MPPT) of individual modules resulting in a substantial power loss during partial shading conditions [1]. Due to higher efficiency and low cost, the family of string inverters has been commercialized on a larger scale. However, these topologies do not possess maximum power point tracking (MPPT) of individual modules resulting in a substantial power loss during partial shading conditions.

Numerous module-based topologies with individual MPPT capability have been proposed for PV application [8] with series and parallel structures as illustrated in Fig.1. For instance, structures proposed in [9], [10], and [11] eliminate the DC/DC conversion stage and all the DC/AC converters in the string are connected in series. The series connections have been effective in achieving the individual MPPT, however, possess the high voltage DC arc fault [12], [13].

To avoid this, parallel structures have been proposed. Despite the series and parallel operation of converter structures, a topology having an isolated DC/AC inverter connected to the module is proposed in [14] and [15] which is termed as microinverter. Besides the mentioned structures, interleaved structures have also proved to be efficient for harvesting maximum power from individual modules [14] but possess increased size and coSt. The transformerless inverter topologies have been reported in [16] and [17]. However, they demand high filter requirements to meet the grid requirements.

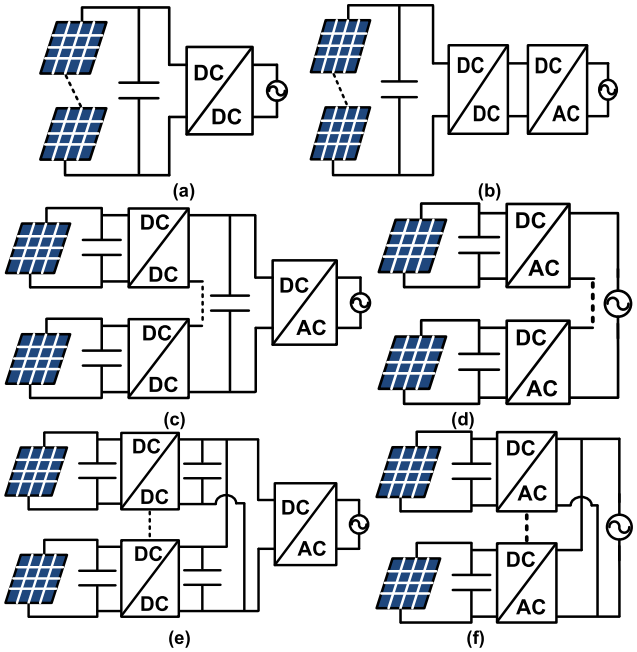

FIGURE 1. Classical Single phase transformerless PV inverters (a) single stage (b) two-stage (c) series connected two stages (d) series connected single stage (e) parallel-connected two stages (f) parallel-connected single stage.

Recent times have witnessed improvement in the transformerless multilevel inverter (MLI) topologies in which cascaded H-bridge (CHB) MLIs have been widely established. A CHB with two modules, each achieving MPPT has been proposed in [9], [10], and [11] with limitations on a maximum number of modules which limits the flexibility for residential applications. To overcome this, a structure with improved flexibility has been proposed using quasi Z-source configuration and connecting it in CHB [18], [19]. However, the additional diodes and the inductors result in decreased efficiency.

The state of art discussed several single-stage and two-stage inverter configurations. The single-stage transformerless MLI structures possess' a low component count and simple structure, however, employ a complex control circuitry for MPPT tracking and voltage regulation. On the other hand, most of the two-stage transformerless MLI structures proved to realize individual MPPT effectively.

A module-based single-phase transformerless MLI for low/medium power PV systems is presented in this paper. The major key features of the converter include:

- The modular structure provides flexibility to increase the number of modules connected
- Less component count
- The controller achieves the dual objective of MPP and grid voltage regulation
- safe limits of leakage currents as per German VDE 0126-1-1 standard

The remaining paper is organized as follows. Section II briefs the system configuration followed by the control strategy in Section III. The systematic design of the controller is discussed in Section IV followed by the simulation results and their discussion in Section V. The experimental results are discussed in Section VI. The qualitative and quantitative comparison of the proposed converter has been discussed in Section VII and finally, Section VIII concludes the paper.

II. SYSTEM CONFIGURATION

The proposed system for the realization of individual MPPT with the controller is depicted in Fig.2. Each module is connected to a switch in series for the MPPT of each PV module and a diode, which bypasses the module when not in operation. The conventional boost converter connected to this enhances the voltage level. The arrangement is further connected to a T-type MLI for five-level voltage generation and then connected to the grid through the filter. It is a well-known fact that MLIs reduce the harmonics and thus the size and cost of the filter. The complete system for better understanding can be divided into three stages. In the first stage, a couple of PV modules are connected in series with self-commutated switches (S_{pv1} *and* S_{pv2}) along with a module bypass diode for each module (D_{pv1} *and* D_{pv2}). The second stage is a conventional boost converter stage with an energy buffer consisting of the filter inductor L_{dc}, self-commutated switch S_{dc} with its anti-parallel diode, a clamping diode D, and filter capacitance C_{dc}. The output stage is the multilevel inverter with the self-commutated switches T_1, T_2, T_3, T_4, and T_5. The output stage is interfaced to load through a low-pass LC filter represented by L_f and C_f. The detailed operation of the first and second stages combinedly

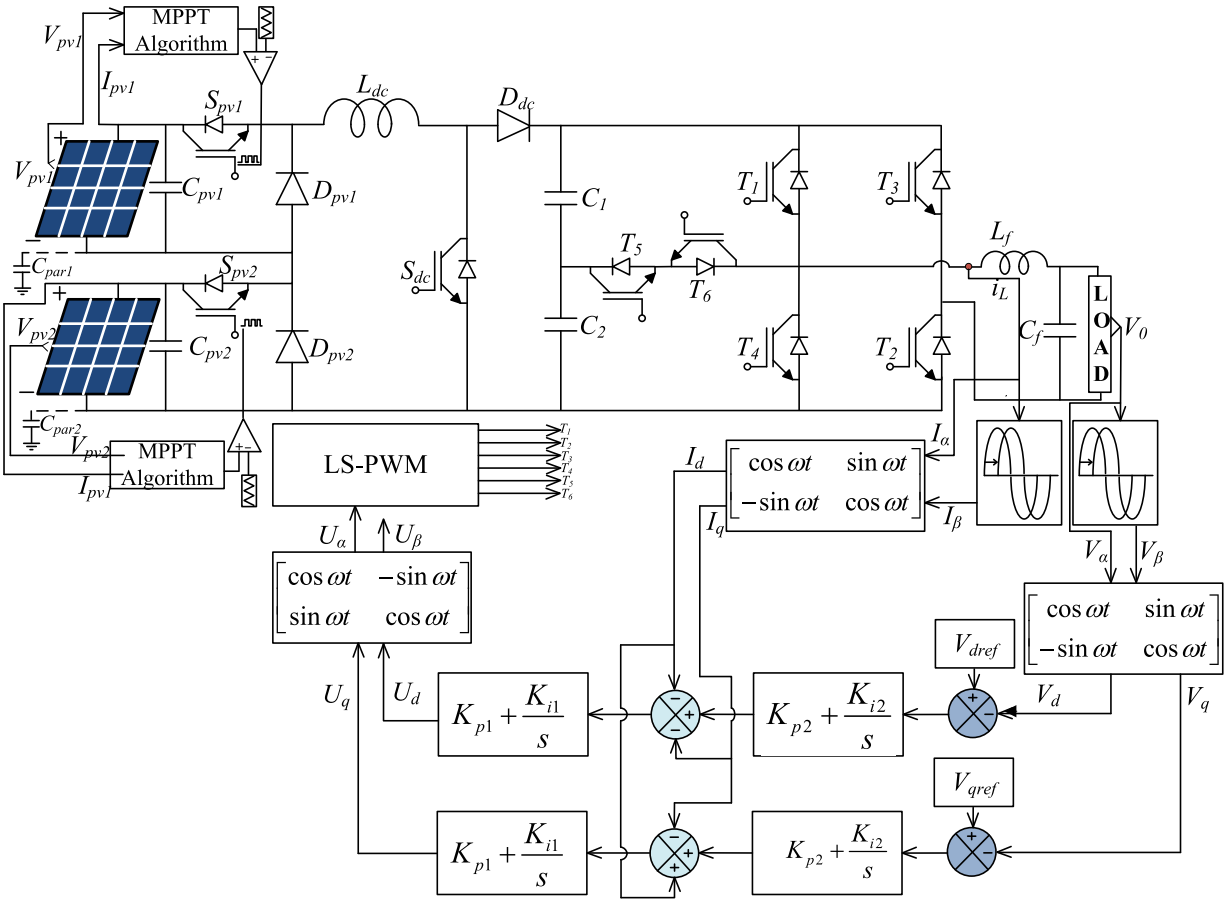

FIGURE 2. Schematic of the proposed configuration with control structure.

is reported in [20]. The third stage is initially proposed in [21] and is well established. The design parameters of the system are listed in Table 1. The sources can be operated either simultaneously or individually. The simultaneous operation results in a series of connections of the modules that make them operate at a common MPP. To avoid such scenarios, a time multiplexing switching scheme has been implemented. The inductor L_{dc}, switch S_{dc} and diode D_{dc} form the conventional boost converter for voltage step-up. The DC/AC conversion using T-type MLI, as mentioned reduces the filter requirements to minimize the switching stress thus enhancing the reliability of the converter. The level-shifted pulse width modulation (LS-PWM) is employed for inherent capacitor voltage balancing.

III. CONTROL STRATEGY

The control technique of the presented system is categorized as MPPT control and Inverter Control. The MPPT control aims in realizing the MPPT of individual modules and the inverter control aims at grid voltage regulation.

A. MPPT CONTROL

To operate each module at individual MPP during partial shading and further to avoid the series operation of the PV modules, the structure is operated with the time multiplexing switching scheme. Owing to the advantages like simple, easier implementation with less computational effort, the classical perturb and observe (P&O) method is employed for MPPT operation [22].

B. INVERTER CONTROL

A pre-defined voltage is desired on the AC side for effective load operations. Numerous inverter control techniques have been discussed in the state of the art for load voltage regulation. Few of them relate to dead beat control [23], virtual impedance-based method [24], and single order decoupled method [25] which have gained high popularity due to their better dynamic performance. In addition, they also give a faster response and can prevent overshoot and ringing if properly designed. However, these are highly sensitive, & complex and moreover do not give zero steady-state error. Synchronous reference frame (SRF) controller exhibits zero steady-state error while achieving improved dynamic performance [26], [27].

The SRF-based PI controller is well established in three-phase systems; however, very limited literature is available for the application of the SRF-PI method for single-phase systems. Owing to the advantage of zero steady-state error,

an attempt has been made to use this method for the proposed grid-connected T-type inverter voltage control. A PLL is employed and regulated for grid frequency control.

C. GENERATION OF ORTHOGONAL PHASE

In three-phase systems, three signals are available for conversion into d-q coordinates using Park's transformation. However, an orthogonal phase is necessary for single-phase systems to provide the d-q frame. Several methods like providing a delay to the original signal [28], differentiating the original signal [29], Hilbert transform [30], and Kalman filter method [31] have been proposed for orthogonal signal generation. For easier implementation, a delay to the original signal is implemented and validated for the proposed converter control. Thus, the original signal along with generated orthogonal signal is used for conversion from $\alpha\beta$ frame to dq frame.

D. CONTROL STRUCTURE

The implemented control structure for the regulation of output voltage is depicted in Fig.2. The scheme consists of an SRFPI-based controller for instantaneous output voltage regulation. For damping and improved transient response, an inner current control loop is provided. In addition to the two loops, a voltage feed-forward path provides the robustness of the system against the possible parameter variation. Implementing an inner current loop includes sensing inductor current which can enable the inverter over current protection.

IV. CONTROLLER DESIGN

Initializing with the orthogonal signal generation, the details of the controller design are followed below:

Step 1: An orthogonal signal ($V\beta$) is generated from the available voltage signal ($V\alpha$).

$$V_\alpha = V_o \sin \omega t \tag{1}$$

$$V_\beta = V_o \sin (\omega t - 90) \tag{2}$$

Step 2: The synchronous reference frame ($\alpha\beta$) is converted to a stationary reference frame (dq) using Park's transformation. The SRF possesses the ability to eliminate the steady-state error by shifting fundamental frequency information back to DC and using a conventional DC regulator such as PI controller. The Park's transformation into a single phase is given by

$$\begin{bmatrix} V_d \\ V_q \end{bmatrix} = \begin{bmatrix} \cos \omega t & \sin \omega t \\ -\sin \omega t & \cos \omega t \end{bmatrix} \begin{bmatrix} V_\alpha \\ V_\beta \end{bmatrix} \tag{3}$$

Step 3: The controller design for the α-frame is discussed and the same is applied to the controller design in the β-frame. The open loop transfer function of the inner loop is given by

$$G_i(s) = \left(\frac{1/L_f}{s + \frac{r_{L_f}}{L_f}} \right) \left(K_{p1} + \frac{K_{i1}}{s} \right) \tag{4}$$

The transfer function magnitude at the gain cross-over frequency is

$$|G_i(j\omega)| = 1 \tag{5}$$

$$\left| \frac{1/L_f}{s + \frac{r_{L_f}}{L_f}} \right| \left| K_{p1} + \frac{K_{i1}}{s} \right| \Bigg|_{s=j\omega_{BWI}} = 1 \tag{6}$$

where ω_{BWO} is the inner loop bandwidth, generally chosen to be one-tenth of the switching frequency (fs) and is given by

$$\omega_{BWO} = \frac{1}{10} * 2\pi f_s rad/\sec . \tag{7}$$

On substituting the converter parameters in (6), an optimization problem is formulated for which the objective function is given as

$$\min(f_1(K_{p1}, K_{i1})) = K_{p1} + (3.18 \times 10^{-4}) K_{i1} - 3.92 \tag{8}$$

The widely used evolutionary optimization technique, genetic algorithm (GA) is implemented to minimize f1. The solution obtained [K_{p1}, K_{i1}] post-convergence of GA is utilized as current controller parameters.

Step 4: The higher bandwidth setting of the inner loop provides a faster response for possible current variations and allows considering the transfer function of the complete inner loop as unity while designing the outer voltage loop parameters. On the same lines as described in step 3, the transfer function is attained from (9) and the objective function is formulated as (10).

$$\left| \frac{1}{Cs} \right| \left| K_{p2} + \frac{K_{i2}}{s} \right| \Bigg|_{s=j\omega_{BWO}} = 1 \tag{9}$$

where ω_{BWO} is the bandwidth of the outer voltage loop and is far less than ω_{BWI}, generally ω_{BWO} is less than one-third of ω_{BWI}.

$$\min(f_2(K_{p2}, K_{i2})) = K_{p2} + (2.5 \times 10^{-4}) K_{i2} - 0.8 (10) \tag{10}$$

Step 5: The quantities in the dq-frame are converted to $\alpha\beta$-frame as

$$\begin{bmatrix} V_\alpha \\ V_\beta \end{bmatrix} = \begin{bmatrix} \cos \omega t & -\sin \omega t \\ \sin \omega t & \cos \omega t \end{bmatrix} \begin{bmatrix} V_d \\ V_q \end{bmatrix} \tag{11}$$

The control output as a reference wave is fed along with the carrier waves to generate switching pulses for the T-type MLI using the LS-PWM switching method.

V. SIMULATION RESULTS

The efficacy of the proposed system and the controller are validated in MATLAB/ Simulink environment under different conditions. In this section, two major conditions, intermittency each on source and load have been considered. The parameters of the 150 W photovoltaic module at standard test conditions (STC) are listed in Table 1 and the design parameters are listed in Table 2.

TABLE 1. Parameters of the 150W module at STC.

Parameter	Value	Parameter	Value
Voc	42.5 V	Vmpp	34.5 V
Isc	5.4 A	Impp	3.5 A

TABLE 2. Design parameters.

Parameter	Value	Parameter	Value
Ldc	2.5 mH	Lf	1 mH
C1	660 µF	Cf	1200 µF
C2	660 µF	fs	10 kHz

Case 1: Intermittency on the source end

Among the numerous possible ways to create intermittency on the source end, imposing partial shading conditions by dissimilar irradiances on the modules has been chosen. To comply with the real-time data, the irradiance at Raipur City of India has been considered. To begin with, both modules were imposed an irradiance level of 821 W/m2. In this condition, the modules were observed to extract a maximum of 120 W each as depicted in Fig.3, which is approximately the MPP, calculated for the respective irradiance level. To impose partial shading conditions, a 25% variation in irradiance level (621 W/m^2) on module 1 has been considered. As observed from Fig.3, module 1 extracts 88 W, which is the approximate respective MPP for the irradiance level. On the other hand, module 2 continues to operate near its MPP (118 W). This verifies that the individual module of the proposed configuration effectively realizes its respective MPP under partial shading. The output of the multilevel inverter and grid voltage is depicted in Fig.4. As observed, the output voltage and the grid voltage remain the same both before and after the partial shading condition. This is due to the controller action which regulates the load voltage during the intermittency on the source end. This validates the effectiveness of the designed controller for the proposed configuration.

Case 2: Intermittency on the load end

The intermittency on the load end has been considered for validating the efficacy of the controller under dynamic loading conditions. A load of 80W is perturbed on the existing 200W load at 0.6s and 0.8s respectively. The voltage and current for dynamic loading are depicted in Fig.5. The increase in load demand increases the current while maintaining a regulated five-level output voltage as depicted in Fig.5(a). During this condition, the controller regulates the load voltage to the reference voltage as illustrated in Fig.5(b). The current fed to the grid is shown in Fig.5(c). This validates the effectiveness of the implemented controller in voltage regulation for intermittencies on the load end.

The leakage current is one of the major issues in grid-connected transformerless inverters. As per German standard VDE 0126-1-1, the leakage current in the inverter should have a magnitude less than 300mA. In this regard, the currents from each PV module to the ground are measured. The measured leakage current and the common mode voltage are depicted in Fig.6 and Fig.7 respectively. It can be observed that the leakage current is far less than the limits thus reflecting the proposed topology satisfies the requirements for grid integration in terms of leakage current. The voltage and current stress of the MLI are depicted in Fig. 8. The control signal from the controller is depicted in Fig. 9.

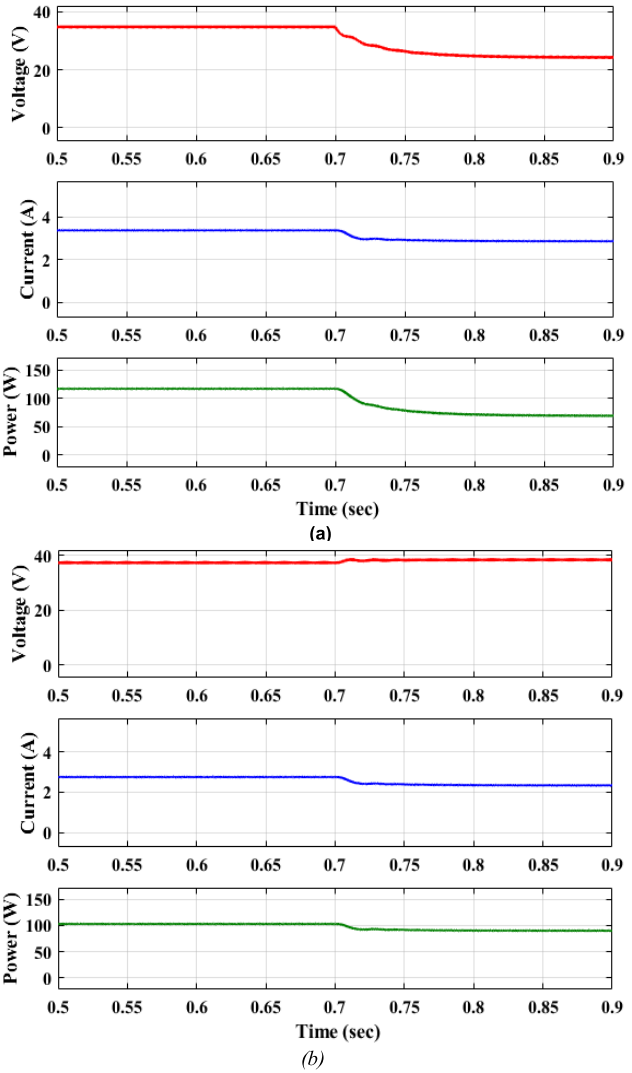

FIGURE 3. Voltage, current and power of (a) module 1 (b) module 2.

VI. EXPERIMENTAL RESULTS

A 300 W laboratory prototype has been developed for experimental validation of the proposed system under source and load intermittencies. The characteristics of the PV modules are replicated by the eco-sense make 1.6kW PV emulator.

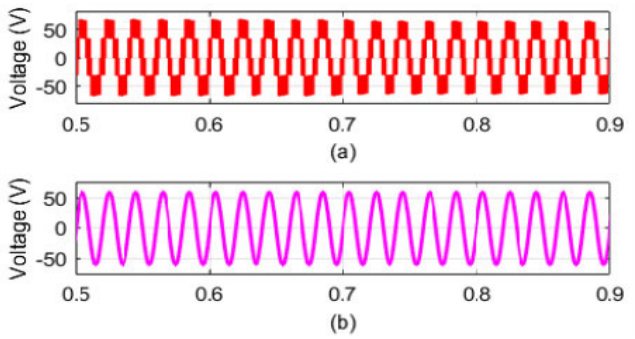

FIGURE 4. (a) Output voltage of the multilevel inverter (b) Grid voltage.

The emulator consists of four independent 400W channels. The emulator provides flexibility for each channel to operate under different irradiances and different locations as well. In this study, Raipur city in India with 21.514oN latitude and 81.6296oE longitude has been considered. The irradiance and temperature of two different periods are fed to a pair of channels in the emulator. The Hall Effect-based LEM LV 25P and LA 55P voltage and current sensors have been used for sensing the voltage and current respectively for MPPT and implementation of the SRF-PI controller. The experimental setup is shown in Fig. 10. The controller is implemented in dSPACE 1103 digital controller. Similar cases as that in the simulation are considered. For source intermittency, a partial shading condition has been imposed on module 1 with a drop in irradiance by 25% i.e., from 821 W/m2 to 611 W/m2. It was observed that the modules operate near the respective MPP as depicted in Fig.11 (a) and (b). The corresponding MLI output voltage, grid voltage, and grid current are depicted in Fig.11 (c).

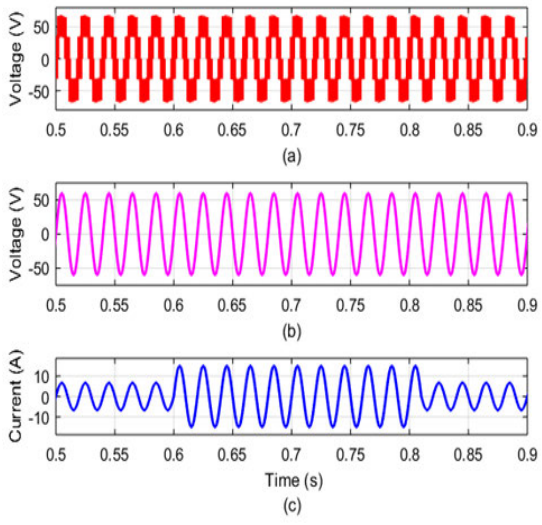

FIGURE 5. (a) T-type inverter output voltage (b) Grid voltage (c) Current fed to the grid.

Further, the performance of the designed controller has been validated with load intermittency. The controller design was

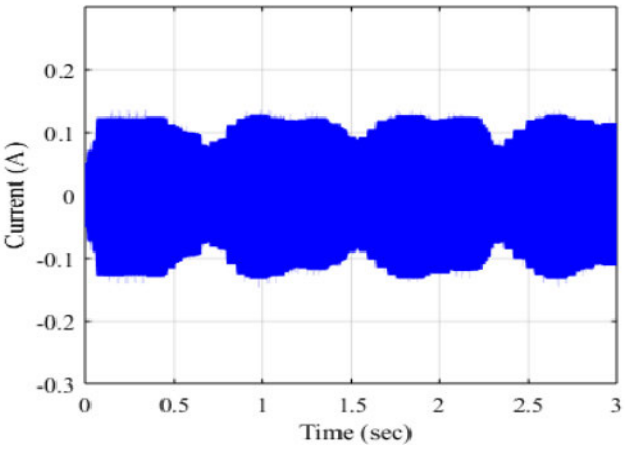

FIGURE 6. Leakage current.

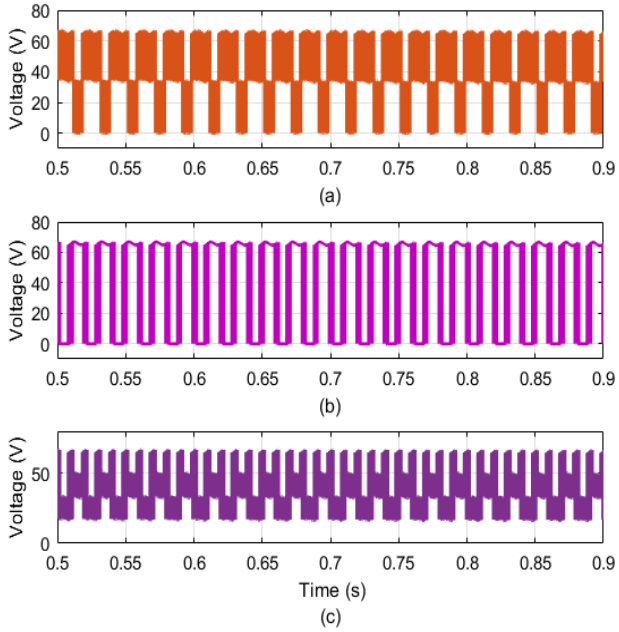

FIGURE 7. (a) VAN (b) VBN (c) Common mode voltage.

robust enough to regulate the inverter voltage and grid voltage at the desired value as depicted in Fig.11.

In addition, to load intermittency, the effectiveness of the controller was also tested for change in reference voltage (grid voltage). With the increase in the grid voltage, the controller regulated the load voltage to near the grid voltage within a very short time as illustrated in Fig.12. With the increase in the reference voltage it is obvious that the grid current also increases as observed from the Fig. 12.

The proposed approach has been validated and proved to be effective in meeting the twin objectives of individual MPP realization and load voltage regulation for source and load intermittencies. However, to verify its viability as a transformerless grid-tied inverter, the leakage current has been measured and observed to be 100mA as depicted in

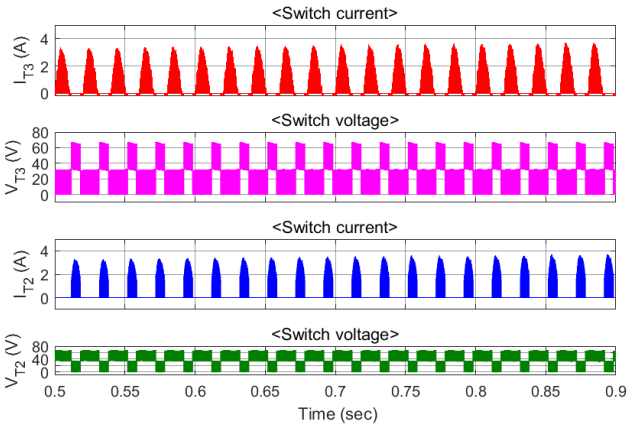

FIGURE 8. Voltage and Current stress across the switches.

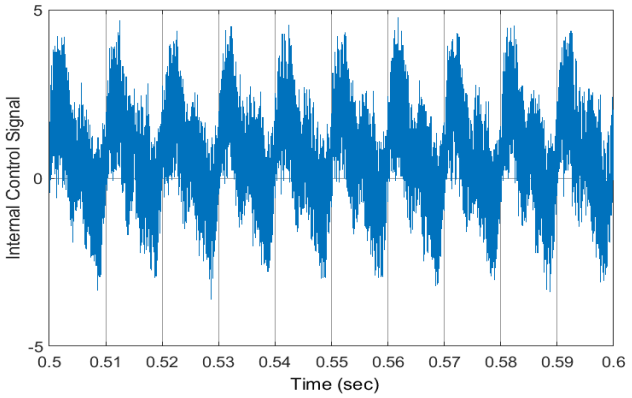

FIGURE 9. Internal Control Signal from the controller.

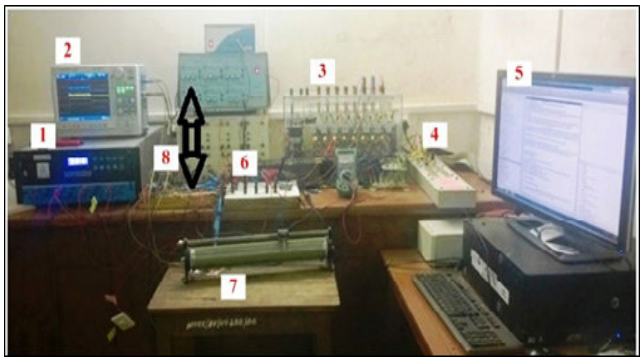

FIGURE 10. Experimental setup 1. PV Emulator 2. Scope corder 3. IGBT module 4. dSPACE 1103 5. Host PC 6. Proposed topology 7. Load 8.Voltage and Current Sensors.

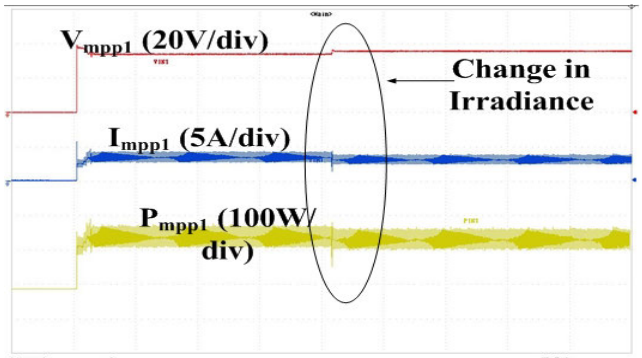

(a)

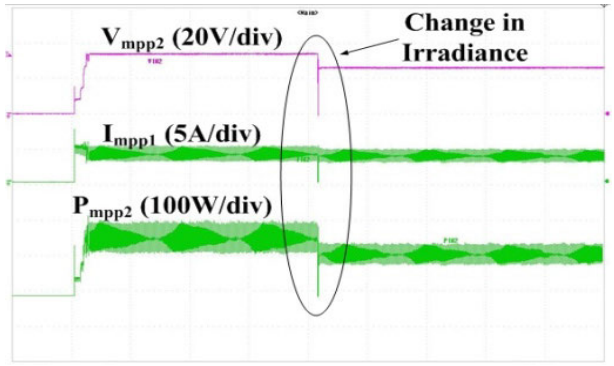

(b)

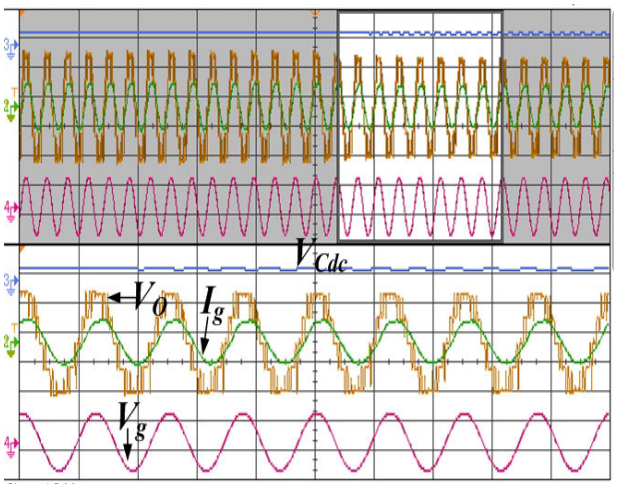

(c)

(Scale: VCdc : 100 V/div; VO : 50 V/div; Ig : 2 A/ div; Vg: 50 V/div, Time:5sec/div)

FIGURE 11. Experimental results under partial shading condition (a) Module 1 (b) module 2 (c) output parameters.

Fig.13 which is less than the 300mA as per the standards. Also, the common voltage has been measured and depicted in Fig.13. Further, as discussed the capacitor has inherent balancing capability under all operating scenarios. The other major issue in multilevel inverters is capacitor balancing. To balance the state of the capacitor voltages, the capacitor voltages at the input of each sub-module of the inverter are measured and depicted in Fig.14. It can be observed that the topology possesses inherent capacitor voltage balancing. The capacitor voltages have measured equal values before and after the irradiance change verifying the inherent balancing property as depicted in Fig.14. The simulation and experimental validation verify that the proposed approach of MIC-based transformerless grid-connected MLI. The MPPT for irradiance has been calculated and validated experimentally. The MPPT tracking efficiency is depicted in Fig. 15.

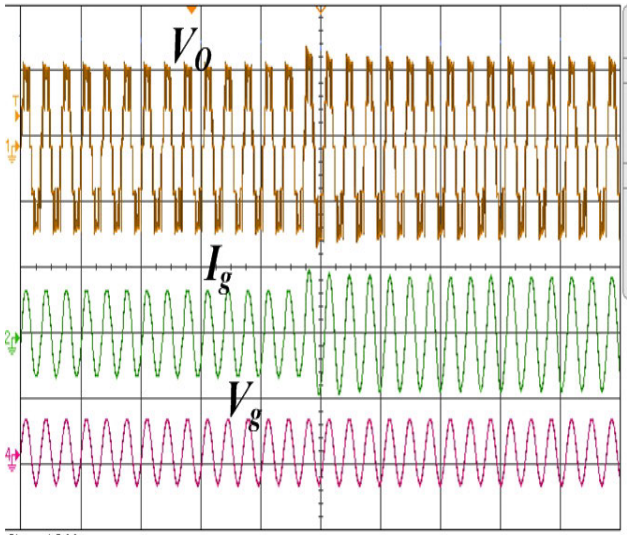

Scale: VO: 50 V/div; Ig: 2 A/ div; Vg: 100 V/div, Time:5sec/div

FIGURE 12. Output parameters under load change.

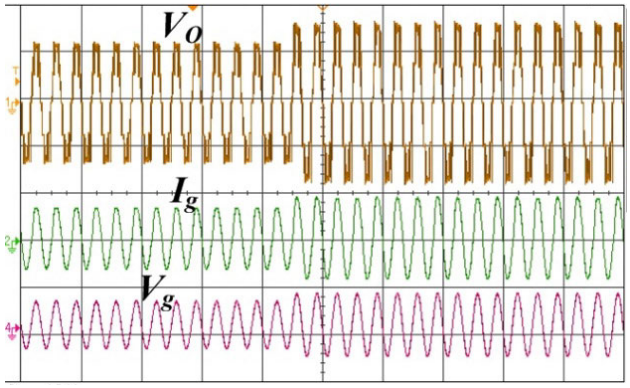

Scale: VO: 50 V/div; Ig: 2 A/ div; Vg: 100 V/div, , Time:5sec/div

FIGURE 13. Output parameters under change in grid reference voltage.

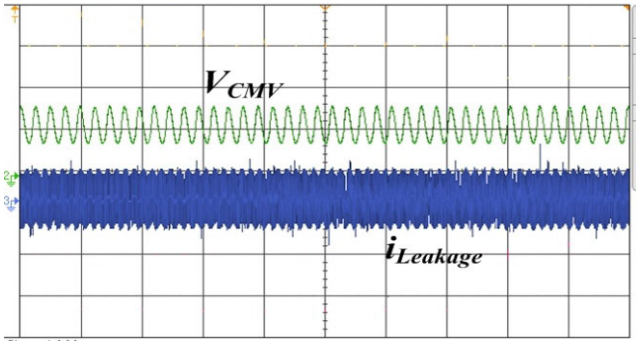

Scale: VCMV: 50V/div; iLeakage: 10mA/div, , Time:5sec/div

FIGURE 14. Common mode voltage and leakage current.

VII. COMPARATIVE ANALYSIS

The proposed converter structure has been qualitatively and quantitatively compared with the recent structures reported in the literature. The qualitative comparison reveals the superiority in simplicity and operating modes. The qualitative comparison is illustrated in Table 3. Results from two recently reported papers have also been included for comparisons [32], [33].

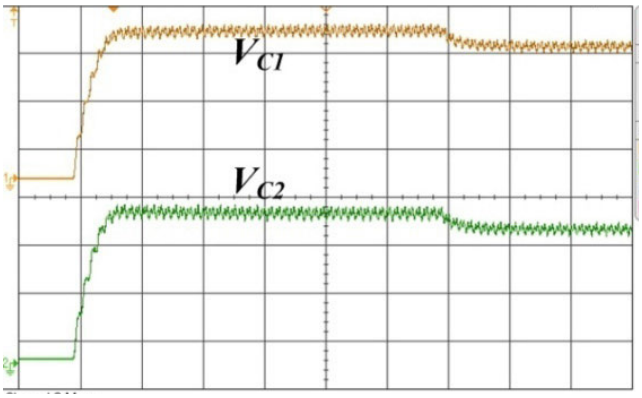

Scale: VC1: 20 V/div and VC2: 20 V/div, , Time:5sec/div

FIGURE 15. Capacitor voltages.

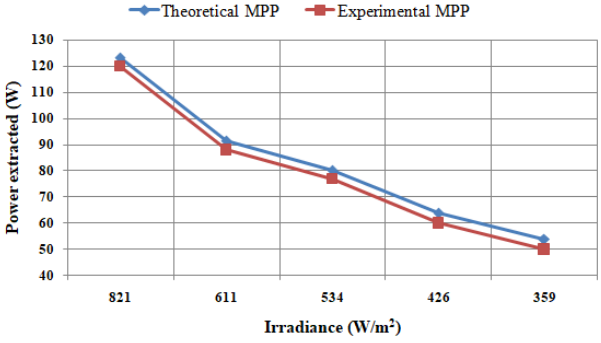

FIGURE 16. MPPT tracking efficiency.

TABLE 3. Qualitative comparison of the proposed topology.

A	B	C	D	E
[14]	1	Yes	High	-
[18]	2	Yes	High	Buck and Boost
[19]	2	Yes	Low	Buck and Boost
[32]_1	2	Yes	Medium	Boost
[32]_2	2	Yes	Medium	Boost
[33]	2	Yes	Medium	Boost
Proposed	2	Yes	Low	Buck, Boost, and Buck-Boost
A- Topology, B- Number of stages involved, C- Realization of Individual MPPT, D- Computational Efforts involved in Controller Design, E- Operating Modes				

Further, the quantitative comparison of the proposed topology with the above topologies for two inputs has been illustrated in Table 4. The topology discussed in [33] employs less number of diodes and capacitors compared to the proposed topology, however, uses more switches comparatively.

TABLE 4. Quantitative comparison of the proposed topology.

Parameter / Topology	No. of Transformers	No. of Diodes	No. of Capacitors	No. of Inductors	No. of Switches	Reported range of efficiency (in %)
[14]	4	4	6	8	8	88-96
[18]	0	2	4	9	9	95-98
[19]	0	2	4	5	8	80-90
[32]_1	0	0	1	2	12	94-98
[32]_2	0	0	1	3	16	94-98
[33]	2	8	8	6	20	95-99
Proposed	0	3	4	2	9	89-95

The topology in [14] has the advantages of single-stage conversion and low switch count when compared to the proposed topology, however, employs more capacitors, diodes, and inductors. The topology in [19] has the advantage of less number of switches and diodes at the cost of inductors resulting in increased size and weight of the system. The total number of components of the proposed topology is far less than that of other topologies discussed. Few topologies use transformers while few others including the proposed do not use the transformer. It can be observed from Table 3 that the control strategy for the proposed topology does not involve more complex computational efforts due to its simple structural design. Also, out of all the discussed topologies, only the proposed converter can be operation modes (buck, boost, and buck-boost).

VIII. CONCLUSION

A transformerless grid-connected photovoltaic multilevel inverter has been proposed in this paper. The proposed system configuration along with the step-by-step design of the control scheme has been discussed. The effectiveness of the controller has been verified under both load and source intermittencies. It was observed that the proposed system achieved the twin objectives of individual MPP realization and voltage regulation for load and source intermittencies. The measured leakage current is only 1mA which is far less than the limit of the German VDE 0126-1-1 standards. Also, the common mode voltage has been validated the proposed converter for its application to the grid-connected systems. Further, the PWM technique and the controller architecture employed inherently balances the capacitor voltages. The method has been validated on the laboratory prototype developed. The overall component count is 18 which is observed to be far less than similar configurations reported in the literature. Also, the converter has proven to have efficiency in the range of 89-95%.

ACKNOWLEDGMENT

This work was supported by the Researchers Supporting Project number (RSPD2023R646), King Saud University, Riyadh, Saudi Arabia.

REFERENCES

[1] J. Hashimoto, T. S. Ustun, M. Suzuki, S. Sugahara, M. Hasegawa, and K. Otani, "Advanced grid integration test platform for increased distributed renewable energy penetration in smart grids," *IEEE Access*, vol. 9, pp. 34040–34053, 2021.
[2] F. Nadeem, M. A. Aftab, S. M. S. Hussain, I. Ali, P. K. Tiwari, A. K. Goswami, and T. S. Ustun, "Virtual power plant management in smart grids with XMPP based IEC 61850 communication," *Energies*, vol. 12, no. 12, p. 2398, Jun. 2019.
[3] G. S. Patil, A. Mulla, S. Dawn, and T. S. Ustun, "Profit maximization with imbalance cost improvement by solar PV-battery hybrid system in deregulated power market," *Energies*, vol. 15, no. 14, p. 5290, Jul. 2022.
[4] S. Odara, Z. Khan, and T. S. Ustun, "Optimizing energy use of SmartFarms with smartgrid integration," in *Proc. 3rd Int. Renew. Sustain. Energy Conf. (IRSEC)*, Marrakech, Morocco, Dec. 2015, pp. 1–6.
[5] J. B. Basu, S. Dawn, P. K. Saha, M. R. Chakraborty, and T. S. Ustun, "A comparative study on system profit maximization of a renewable combined deregulated power system," *Electronics*, vol. 11, no. 18, p. 2857, Sep. 2022.
[6] K. A. Mahafzah, M. A. Obeidat, A. Q. Al-Shetwi, and T. S. Ustun, "A novel synchronized multiple output DC–DC converter based on hybrid flyback-cuk topologies," *Batteries*, vol. 8, no. 8, p. 93, Aug. 2022.
[7] W. Li, Y. Gu, H. Luo, W. Cui, X. He, and C. Xia, "Topology review and derivation methodology of single-phase transformerless photovoltaic inverters for leakage current suppression," *IEEE Trans. Ind. Electron.*, vol. 62, no. 7, pp. 4537–4551, Jul. 2015, doi: 10.1109/TIE.2015.2399278.
[8] B. York, W. Yu, and J. Lai, "An integrated boost resonant converter for photovoltaic applications," *IEEE Trans. Power Electron.*, vol. 28, no. 3, pp. 1199–1207, Mar. 2013, doi: 10.1109/TPEL.2012.2207127.
[9] B. Xiao, L. Hang, J. Mei, C. Riley, L. M. Tolbert, and B. Ozpineci, "Modular cascaded H-bridge multilevel PV inverter with distributed MPPT for grid-connected applications," *IEEE Trans. Ind. Appl.*, vol. 51, no. 2, pp. 1722–1731, Mar. 2015, doi: 10.1109/TIA.2014.2354396.
[10] Q. Huang, W. Yu, and A. Q. Huang, "Independent DC link voltage control of cascaded multilevel PV inverter," in *Proc. IEEE Appl. Power Electron. Conf. Expo. (APEC)*, Mar. 2016, pp. 2727–2734, doi: 10.1109/APEC.2016.7468249.
[11] J. Chavarría, D. Biel, F. Guinjoan, C. Meza, and J. J. Negroni, "Energy-balance control of PV cascaded multilevel grid-connected inverters under level-shifted and phase-shifted PWMs," *IEEE Trans. Ind. Electron.*, vol. 60, no. 1, pp. 98–111, Jan. 2013, doi: 10.1109/TIE.2012.2186108.
[12] J. Johnson, M. Montoya, S. McCalmont, G. Katzir, F. Fuks, J. Earle, A. Fresquez, S. Gonzalez, and J. Granata, "Differentiating series and parallel photovoltaic arc-faults," in *Proc. 38th IEEE Photovolt. Spec. Conf.*, Jun. 2012, pp. 720–726, doi: 10.1109/PVSC.2012.6317708.
[13] M. K. Alam, F. Khan, J. Johnson, and J. Flicker, "A comprehensive review of catastrophic faults in PV arrays: Types, detection, and mitigation techniques," *IEEE J. Photovolt.*, vol. 5, no. 3, pp. 982–997, May 2015, doi: 10.1109/JPHOTOV.2015.2397599.
[14] M. A. Rezaei, K. Lee, and A. Q. Huang, "A high-efficiency flyback micro-inverter with a new adaptive snubber for photovoltaic applications," *IEEE Trans. Power Electron.*, vol. 31, no. 1, pp. 318–327, Jan. 2016, doi: 10.1109/TPEL.2015.2407405.
[15] J. T. Stauth, M. D. Seeman, and K. Kesarwani, "Resonant switched-capacitor converters for sub-module distributed photovoltaic power management," *IEEE Trans. Power Electron.*, vol. 28, no. 3, pp. 1189–1198, Mar. 2013, doi: 10.1109/TPEL.2012.2206056.
[16] P. K. Chamarthi, M. S. El Moursi, V. Khadkikar, K. H. A. Hosani, and T. H. M. El-Fouly, "Novel step-up transformerless inverter topology for 1-F grid-connected photovoltaic system," *IEEE Trans. Ind. Appl.*, vol. 57, no. 3, pp. 2801–2815, May 2021, doi: 10.1109/TIA.2021.3066141.
[17] S. Gangavarapu, M. Verma, and A. K. Rathore, "A novel transformerless single-stage grid-connected solar inverter," *IEEE J. Emerg. Sel. Topics Power Electron.*, vol. 11, no. 1, pp. 970–980, Feb. 2023, doi: 10.1109/JESTPE.2020.3007556.
[18] Y. Zhou, L. Liu, and H. Li, "A high-performance photovoltaic module-integrated converter (MIC) based on cascaded quasi-Z-source inverters (qZSI) using eGaN FETs," *IEEE Trans. Power Electron.*, vol. 28, no. 6, pp. 2727–2738, Jun. 2013, doi: 10.1109/TPEL.2012.2219556.
[19] D. Sun, B. Ge, X. Yan, D. Bi, H. Zhang, Y. Liu, H. Abu-Rub, L. Ben-Brahim, and F. Z. Peng, "Modeling, impedance design, and efficiency analysis of quasi-Z source module in cascaded multilevel photovoltaic power system," *IEEE Trans. Ind. Electron.*, vol. 61, no. 11, pp. 6108–6117, Nov. 2014, doi: 10.1109/tie.2014.2304913.

[20] A. H. Chander and L. Kumar, "MIC for reliable and efficient harvesting of solar energy," *IET Power Electron.*, vol. 12, no. 2, pp. 267–275, Feb. 2019, doi: 10.1049/iet-pel.2018.5079.
[21] M. Schweizer and J. W. Kolar, "Design and implementation of a highly efficient three-level T-type converter for low-voltage applications," *IEEE Trans. Power Electron.*, vol. 28, no. 2, pp. 899–907, Feb. 2013, doi: 10.1109/TPEL.2012.2203151.
[22] A. A. Elbaset, H. Ali, M. Abd-El-Sattar, and M. Khaled, "Implementation of a modified perturb and observe maximum power point tracking algorithm for photovoltaic system using an embedded microcontroller," *IET Renew. Power Gener.*, vol. 10, no. 4, pp. 551–560, Apr. 2016, doi: 10.1049/iet-rpg.2015.0309.
[23] A. Kawamura and K. Ishihara, "Real time digital feedback control of three phase PWM inverter with quick transient response suitable for uninterruptible power supply," in *Proc. IEEE Ind. Appl. Soc. Annu. Meeting*, Oct. 1988, pp. 728–734, doi: 10.1109/IAS.1988.25143.
[24] J. Chen, D. Yue, C. Dou, L. Chen, S. Weng, and Y. Li, "A virtual complex impedance based $P - \dot{V}$ droop method for parallel-connected inverters in low-voltage AC microgrids," *IEEE Trans. Ind. Informat.*, vol. 17, no. 3, pp. 1763–1773, Mar. 2021, doi: 10.1109/TII.2020.2997054.
[25] N. Mukundan C. M., S. B. Q. Naqvi, B. Singh, and P. Jayaprakash, "Single-layer decoupled multiple-order generalized integral control for single-stage solar energy grid integrator with maximum power extraction," *IEEE Trans. Ind. Informat.*, vol. 17, no. 1, pp. 100–109, Jan. 2021.
[26] M. J. Ryan and R. D. Lorenz, "Synchronous-frame controller for a single-phase sine wave inverter," *Proc. IEEE Appl. Power Electron. Conf. Expo. (APEC)*, vol. 2, Feb. 1997, pp. 813–819, doi: 10.1109/APEC.1997.575739.
[27] M. Monfared, S. Golestan, and J. M. Guerrero, "Analysis, design, and experimental verification of a synchronous reference frame voltage control for single-phase inverters," *IEEE Trans. Ind. Electron.*, vol. 61, no. 1, pp. 258–269, Jan. 2014, doi: 10.1109/TIE.2013.2238878.
[28] R. Zhang, M. Cardinal, P. Szczesny, and M. Dame, "A grid simulator with control of single-phase power converters in D-Q rotating frame," in *Proc. Rec. Annu. Power Electron. Spec. Conf. (PESC)*, vol. 3, 2002, pp. 1431–1437, doi: 10.1109/PSEC.2002.1022377.
[29] A. Roshan, R. Burgos, A. C. Baisden, F. Wang, and D. Boroyevich, "A D-Q frame controller for a full-bridge single phase inverter used in small distributed power generation systems," in *Proc. 22nd Annu. IEEE Appl. Power Electron. Conf. Expo. (APEC)*, Feb. 2007, pp. 641–647, doi: 10.1109/APEX.2007.357582.
[30] M. Saitou and T. Shimizu, "Generalized theory of instantaneous active and reactive powers in single-phase circuits based on Hilbert transform," in *Proc. IEEE 33rd Annu. IEEE Power Electron. Specialists Conf.*, no. 2, Jun. 2002, pp. 1419–1424, doi: 10.1109/PSEC.2002.1022375.
[31] M. Ciobotaru, R. Teodorescu, and F. Blaabjerg, "A new single-phase PLL structure based on second order generalized integrator," in *Proc. 37th IEEE Power Electron. Spec. Conf. (PESC)*, Jun. 2006, pp. 1–6, doi: 10.1109/PESC.2006.1711988.
[32] Q. Huang, A. Q. Huang, R. Yu, P. Liu, and W. Yu, "High-efficiency and high-density single-phase dual-mode cascaded buck–boost multilevel transformerless PV inverter with GaN AC switches," *IEEE Trans. Power Electron.*, vol. 34, no. 8, pp. 7474–7488, Aug. 2019, doi: 10.1109/TPEL.2018.2878586.
[33] Z. Zhang, J. Zhang, S. Shao, and J. Zhang, "A high-efficiency single-phase T-type BCM microinverter," *IEEE Trans. Power Electron.*, vol. 34, no. 1, pp. 984–995, Jan. 2019, doi: 10.1109/TPEL.2018.2824342.

ALLAMSETTY HEMA CHANDER is currently an Assistant Professor with the Department of Electrical and Electronics Engineering, National Institute of Technology Puducherry, India. His current research interests include power electronic converters for renewable energy and electric vehicle applications and battery management systems.

K. DHANANJAY RAO received the M.E. degree in electrical engineering from Jadavpur University, Kolkata, India, and the Ph.D. degree in electrical engineering from the National Institute of Technology, Raipur, India. He is currently an Assistant Professor with the Velagapudi Ramakrishna Siddhartha College of Engineering, Vijayawada, India. His research interests include energy storage devices, fractional-order modeling, and control systems.

BANKUPALLI PHANI TEJA received the B.Tech. and M.Tech. degrees from Jawaharlal Nehru Technological University, Kakinada, India, in 2012 and 2015, respectively. He was a Junior Research Fellow with the National Institute of Technology, Raipur, India. He is currently an Assistant Professor with the Aditya Institute of Technology and Management, Tekkali, India. His current research interests include power electronic converters for fuel cells, electrical drives, and hybrid energy systems.

LALIT KUMAR SAHU (Member, IEEE) received the M.Tech. and Ph.D. degrees from the Maulana Azad National Institute of Technology (MANIT), Bhopal, India, in 2010 and 2016, respectively. He is currently an Assistant Professor with the Department of Electrical Engineering, National Institute of Technology, Raipur, India. His research interests include power electronic converters, electrical drives, electric and hybrid electric vehicular systems, and renewable and hybrid energy systems.

SUBHOJIT DAWN received the M.Tech. degree in power and energy systems engineering and the Ph.D. degree in electrical engineering from the National Institute of Technology Silchar, India. He is currently an Assistant Professor with the Electrical and Electronics Engineering Department, Velagapudi Ramakrishna Siddhartha Engineering College, India. His current research interests include power system economics, renewable energy integration, power system planning, congestion management, smart grids, the electricity market, and energy management.

FAISAL ALSAIF graduated with B.Sc. in electrical engineering from King Saud University in Riyadh, Saudi Arabia, in 2014, and M.A.Sc. in electrical engineering from The Ohio State University, Ohio, USA, in 2017, and the Ph.D. degree in electrical engineering from The Ohio State University, Ohio, USA, in 2022. He is currently working as an Assistant Professor with the Department of Electrical Engineering, College of Engineering, King Saud University, Riyadh, Saudi Arabia. His research interests include power and energy, power electronics, high voltage, smart grids and power quality improvement.

SAGER ALSULAMY received the M.Sc. degree in electrical engineering from the University of Southern California, in 2016, with a focus on renewable energy and climate change. His Ph.D. research involves energy decarbonization pathways for newly built cities in Saudi Arabia. He is a Postgraduate Research Student. During his master's studies, he has participated in smart grid regional demonstration projects and electrical vehicle programs. His previous experience includes working in the utility as an electrical engineer in the distribution sector, testing and commissioning high to medium-voltage substations, and routine and type tests for different electrical network equipment, such as cables, transformers, circuit breakers, and overhead lines. His current research interest includes developing a low-carbon transition pathways plan for a non-grid-connected case study city in Saudi Arabia.

TAHA SELIM USTUN (Member, IEEE) received the Ph.D. degree in electrical engineering from Victoria University, Melbourne, VIC, Australia. He is currently a Researcher with the Fukushima Renewable Energy Institute (FREA), National Institute of Advanced Industrial Science and Technology (AIST), where he leads the Smart Grid Cybersecurity Laboratory. Before that, he was a Faculty Member of the School of Electrical and Computer Engineering, Carnegie Mellon University, Pittsburgh, PA, USA. He has been invited to run specialist courses in Africa, India, and China. His research has attracted funding from prestigious programs in Japan, Australia, Europe, and North America. His current research interests include power systems protection, communication in power networks, distributed generation, microgrids, electric vehicle integration, and cybersecurity in smart grids. He is a member of the IEC Renewable Energy Management WG8 and IEC TC 57 WG17. He has delivered talks at the Qatar Foundation, the World Energy Council, the Waterloo Global Science Initiative, and the European Union Energy Initiative (EUEI). He also serves on the editorial board of IEEE Access, IEEE Transactions on Industrial Informatics, *Energies*, *Electronics*, *Electricity*, *World Electric Vehicle Journal*, and *Information* journal.